Spectrum of Engineering Sciences
ISSN (e) 3007-3138 (p) 3007-312X Volume 4, Issue 3, 2026

PHYTOCHEMICAL-MEDIATED GREEN SYNTHESIS OF TiO_2 NANOPARTICLES USING SOLANUM SURATTENSE: CHARACTERIZATION AND ANTIMICROBIAL ACTIVITY

Sundas khan[1], Umme Farwa Shabeer[2], Isma Bibi[3], Muhammad Atif Khan[4], Anees Khatoon[5], Asad Zamir[*6], Afshan Farooq[7], Maaz Khan[8]

[1] *National center of excellence in physical chemistry, University of Peshawar, Pakistan*
[2] *Department of Chemistry, Government College University Faisalabad, Pakistan*
[3] *Department of Chemistry, Govt. Girls Post Graduate College Bhimber, AZ Kashmir, Pakistan*
[4] *Institute of Chemical Sciences, Gomal University, Dera Ismail Khan Pakistan*
[5] *Liaquat university of Medical and health sciences, Jamshoro, Pakistan*
[6] *Department of Chemistry, Government Post Graduate College Karak, Pakistan*
[7] *Department of Chemistry, Kohat University of Science and Technology, Kohat KP, Pakistan*
[8] *Department of Chemistry, University of Malakand, Dir Lower, Khyber Pakhtunkhwa, Pakistan*

[1] sundaskhan1812000@gmail.com, [2] farwashabeer80@gmail.com, [3] ismaa3345@gmail.com, [4] atifk7748@gmail.com, [5] aneeskhatoon536@gmail.com, [*6] asadzamir000@gmail.com, [7] afshanfarooq211@gmail.com, [8] maazkhanchem@gmail.com

DOI: https://doi.org/10.5281/zenodo.21295102

Keywords
Solanum surattense; Titanium dioxide nanoparticles; Green synthesis; Solasodine; Flavonoids; Antimicrobial activity

Article History
Received: 30 January 2026
Accepted: 06 March 2026
Published: 31 March 2026

Corresponding Author: *
Asad Zamir

Abstract
An eco-friendly and cost-effective approach was developed for the green synthesis of titanium dioxide nanoparticles (TiO_2 NPs) using solasodine- and flavonoid-rich Solanum surattense extract as a natural phytochemical medium. Optimal synthesis was achieved using 10 mL of extract at 60 °C for 2 h and pH 7. UV–visible spectroscopy revealed a characteristic absorption peak at approximately 244 nm, while X-ray diffraction confirmed highly crystalline anatase-phase TiO_2 with an average crystallite size of 19.69 nm. Scanning electron microscopy showed predominantly spherical, aggregated particles ranging from 10 to 80 nm. The synthesized TiO_2 NPs exhibited notable antimicrobial activity against Staphylococcus aureus and Aspergillus fumigatus, producing inhibition zones of 18 ± 0.5 and 17 ± 0.4 mm, respectively, substantially exceeding those of the crude extract. These findings demonstrate a sustainable route for producing phytochemical-mediated TiO_2 NPs with promising antimicrobial and broader multifunctional applications.

INTRODUCTION

Nanotechnology has transformed modern materials science by making it possible to control and modify matter at dimensions generally ranging from 1 to 100 nm (Bayda et al., 2020). Within this size range, materials often develop physicochemical properties that are substantially different from those of their bulk counterparts (Maaz et al., 2024). These include a higher surface-area-to-volume ratio, greater surface reactivity, and unique optical and catalytic behaviour (Ur Rehman et al., 2024). Among the wide range of nanomaterials studied to date, titanium dioxide nanoparticles (TiO_2 NPs) have received considerable interest because of their high chemical stability, strong photocatalytic performance, biocompatibility, affordability, and broad-spectrum antimicrobial potential (Verma et al., 2022).

TiO_2 mainly occurs in three crystalline forms: anatase, rutile, and brookite (Diebold, 2003). Of these phases, anatase is especially valuable for photocatalytic and antimicrobial purposes because of its greater surface activity and ability to generate reactive oxygen species (ROS) efficiently (Prakash et al., 2018). When reduced to the nanoscale, TiO_2 offers a much larger active surface area, which promotes stronger interactions with microbial cells and environmental contaminants. Owing to these characteristics, TiO_2 NPs are considered promising materials for a variety of applications, including antimicrobial coatings, biomedical systems, wastewater treatment, photocatalytic degradation, food packaging, and environmental remediation (Rathore et al., 2023).

Despite these advantages, conventional techniques used for the synthesis of TiO_2 NPs often depend on hazardous chemicals, organic solvents, highly acidic or alkaline reaction conditions, and processes that consume substantial amounts of energy (Rekha et al., 2024). Many physical and chemical synthesis routes also require sophisticated equipment and may produce harmful by-products (Hussain et al., 2026). Such drawbacks have increased interest in greener synthesis strategies that employ biological resources, particularly plant extracts, as natural phytochemical-based systems for nanoparticle formation, capping, and stabilization (Verma et al., 2022).

Plant-based synthesis provides several important benefits compared with conventional nanoparticle production methods (Jan et al., 2025). It minimizes the need for hazardous chemicals, can be carried out under relatively mild reaction conditions, consumes less energy, and allows natural stabilization of nanoparticle surfaces through phytochemical capping (Nurudeen et al., 2025). In addition, the involvement of plant-derived compounds may enhance the biological properties of the resulting nanoparticles (Singh et al., 2023). Plant extracts are naturally rich in various bioactive constituents, such as flavonoids, alkaloids, phenolic compounds, terpenoids, proteins, and reducing sugars (Abbasi et al., 2026). These phytochemicals can interact with nanoparticle precursor species and participate in important stages of synthesis, including nucleation, control of particle growth, surface capping, and stabilization (Villagrán et al., 2024).

Solanum surattense, a medicinal plant of the family Solanaceae, represents a promising biological source for the green synthesis of TiO_2 NPs (Mohany et al., 2023). The plant contains a wide range of biologically active phytochemicals, particularly the steroidal alkaloid solasodine and several flavonoid compounds (Alalwiat et al., 2025). The functional groups present in these constituents can interact with titanium precursor species and may support nanoparticle formation. At the same time, they can form a phytochemical coating around the nanoparticles, helping to limit excessive aggregation (Tekuri et al., 2019). The retention of these bioactive compounds on the nanoparticle surface may also contribute to improved antimicrobial activity through possible synergistic effects.

The present study investigates the potential of solasodine- and flavonoid-rich *S. surattense* extract as a green phytochemical medium for producing multifunctional TiO_2 NPs. Accordingly, the study aims to synthesize TiO_2 NPs using *S. surattense* extract through an optimized green synthesis approach and to characterize the resulting nanoparticles by UV–Vis spectroscopy, X-ray diffraction (XRD), and scanning electron microscopy (SEM). Their antimicrobial activity against *Staphylococcus aureus* and *Aspergillus fumigatus* is also evaluated in comparison with standard antimicrobial agents. Furthermore, the study explores the broader multifunctional potential of the synthesized TiO_2 NPs for biomedical and environmental applications.

MATERIALS AND METHODS

2.1 Plant Material and Extract Preparation

Fresh, healthy *Solanum surattense* plant material was collected and washed thoroughly with distilled water to eliminate dust and other surface contaminants. The cleaned plant material was then dried in the shade for 7–10 days before being ground into a fine powder. For preparation of the aqueous extract, 10 g of the dried powder was mixed with 100 mL of distilled water and heated at 80 °C for 20 min under continuous stirring. The mixture was allowed to cool to room temperature and subsequently filtered through Whatman No. 1 filter paper. The resulting clear filtrate, rich in solasodine, flavonoids, and other plant-derived phytochemicals, was collected and stored at 4 °C until further use in the green synthesis of TiO_2 nanoparticles. The complete procedure used to prepare the aqueous *S. surattense* extract is presented in Figure 1.

Figure 1. Schematic representation of the preparation of aqueous Solanum surattense extract for the green synthesis of TiO_2 nanoparticles.

Green Synthesis of Titanium Dioxide Nanoparticles

A 50 mL aqueous solution of the titanium precursor was first prepared. Subsequently, 10 mL of *Solanum surattense* extract was slowly introduced into the precursor solution while the mixture was continuously stirred using a magnetic stirrer. The reaction was maintained at 60 °C for 2 h. The initial formation of TiO_2 nanoparticles was indicated by a noticeable change in the appearance of the reaction mixture, together with the development of a whitish suspension. The resulting suspension was then centrifuged at 10,000 rpm for 15 min. The collected precipitate was washed three times with distilled water to remove residual precursor and loosely bound phytochemicals. After purification, the product was dried at 60 °C to obtain *S. surattense*-mediated TiO_2 nanoparticles, which were subsequently used for characterization and antimicrobial assessment. The complete green synthesis process is illustrated in Figure 2.

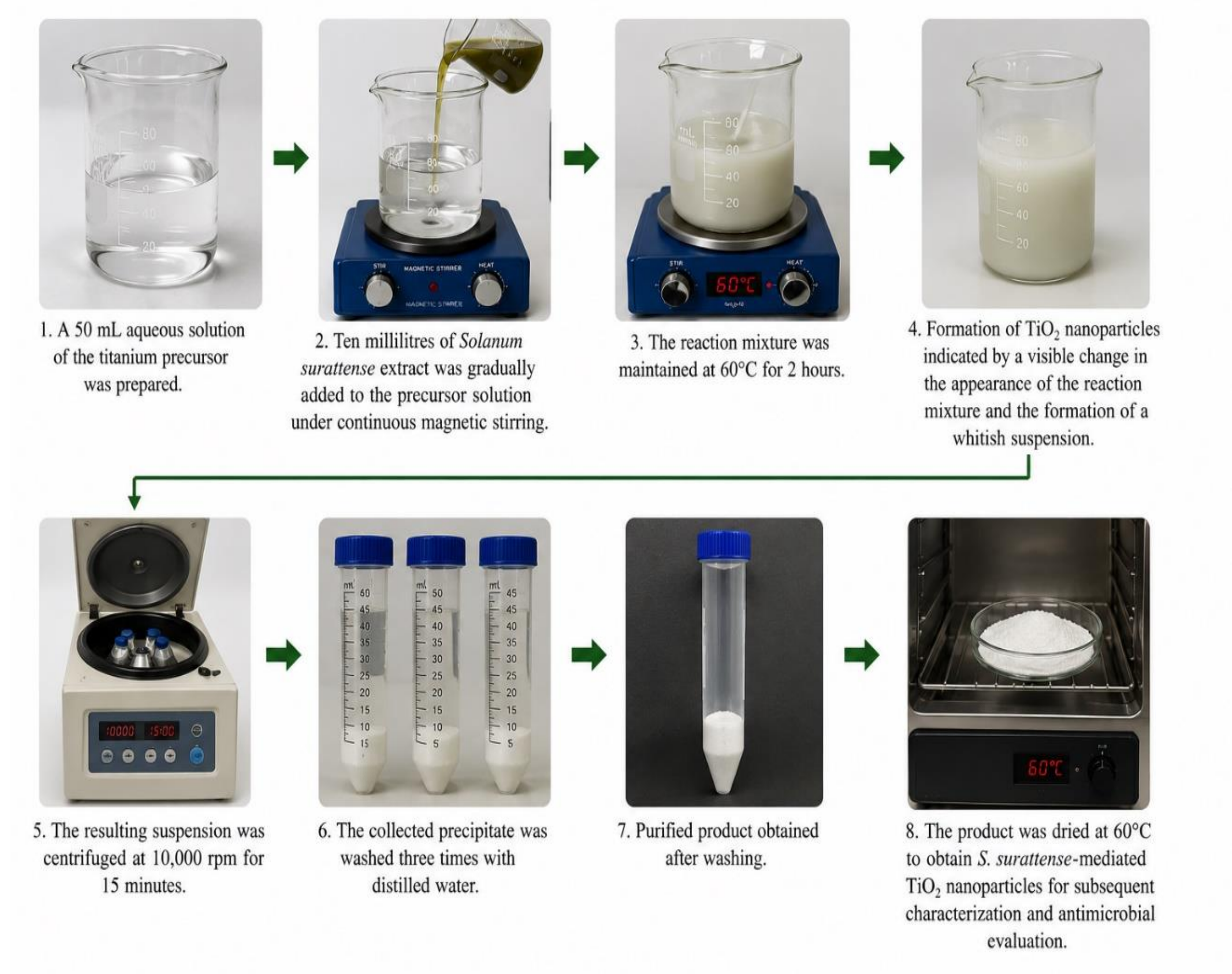

Figure 2 Green Synthesis of Titanium Dioxide Nanoparticles.

2.3 Optimization Studies

The synthesis conditions were optimized by examining the influence of several experimental parameters, including the volume of *Solanum surattense* extract (5, 10, and 15 mL), reaction temperature (40, 60, and 80 °C), reaction duration (30 min to 3 h), and pH (5, 7, and 9). The most appropriate conditions were selected by considering the extent of nanoparticle formation, product yield, stability, and particle uniformity. Throughout the optimization process, visible changes in the reaction mixture and its stability were carefully monitored. The conditions identified as optimal were then applied to synthesize TiO_2 nanoparticles for subsequent physicochemical characterization and antimicrobial assessment.

2.4 Characterization

The optical properties of the green-synthesized TiO_2 nanoparticles were examined using a double-beam UV–Vis spectrophotometer over a wavelength range of 200–800 nm. The crystalline structure and phase composition of the synthesized TiO_2 nanoparticles were analyzed using an X-ray diffractometer with Cu-Kα radiation (λ = 1.5406 Å) over a 2θ range of 10–80°. The average crystallite size was calculated using the Debye–Scherrer equation:

$$D = \frac{K\lambda}{\beta \cos\theta}$$

The morphology, surface characteristics, and particle-size distribution of the TiO_2 nanoparticles were examined using SEM. The average particle diameter was determined by measuring 100 randomly selected particles from the micrographs using ImageJ software.

2.5 Antimicrobial Activity Assay

The antimicrobial activity of the synthesized nanoparticles was examined by the agar well diffusion method against *Staphylococcus aureus*, a Gram-positive bacterium, and *Aspergillus fumigatus*, a pathogenic fungus. Nutrient agar was used for bacterial cultivation, whereas potato dextrose agar was prepared for fungal growth, and both media were sterilized before use. A standardized microbial suspension containing approximately 4 × 10^2 CFU/mL was evenly spread over the surface of the solidified agar plates. Using a sterile cork borer, wells measuring 6–8 mm in diameter were made and loaded with 60–100 µL of the respective test samples. These included *S. surattense*-mediated TiO_2 NPs, crude *S. surattense* extract, amoxicillin as the antibacterial positive control, clotrimazole as the antifungal positive control, and sterile water as the negative control. The inoculated plates were incubated at 35 °C for 18–24 h, after which the resulting zones of inhibition were measured with a digital caliper. The complete experimental procedure used to assess antimicrobial activity is presented in Figure 3.

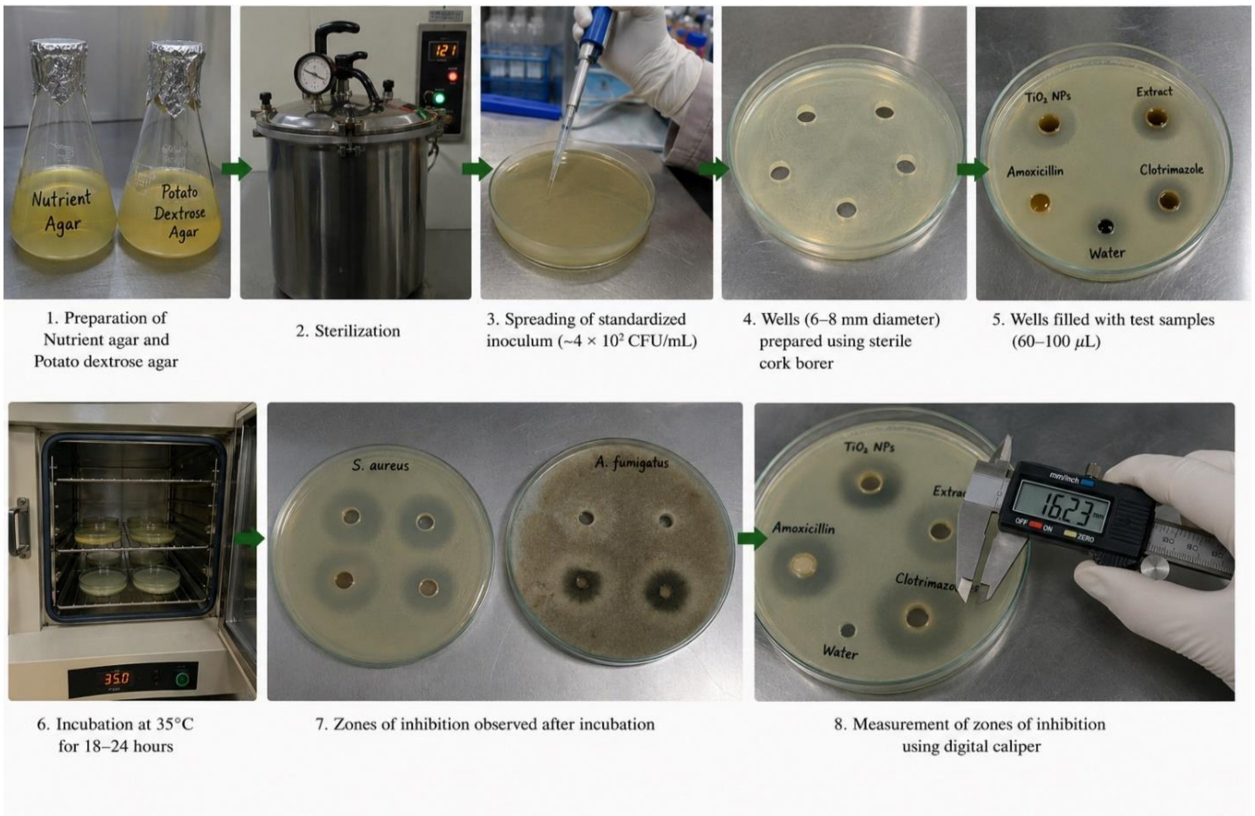

Figure 3. Agar well diffusion assay for antimicrobial evaluation of Solanum surattense-mediated TiO_2 nanoparticles.

Statistical Analysis

All experiments were conducted in triplicate. Data were expressed as mean ± standard deviation (SD). Statistical comparisons between the green-synthesized TiO_2 NPs, crude *Solanum surattense* extract, and positive controls were performed using Student's *t*-test. A *p*-value of less than 0.05 ($p < 0.05$) was considered statistically significant.

RESULTS AND DISCUSSION

Visual Observation of Nanoparticle Formation

The initial formation of TiO_2 nanoparticles was indicated by a clear change in the appearance of the reaction mixture after *Solanum surattense* extract was added to the titanium precursor solution. During incubation at 60 °C for 2 h, the initially clear solution gradually developed into a whitish and turbid suspension, suggesting the formation of TiO_2 particles. The phytochemical constituents of *S. surattense*, particularly solasodine, flavonoids, and phenolic compounds, are believed to interact with the titanium precursor species and assist different stages of nanoparticle formation, including hydrolysis, nucleation, particle growth, and surface stabilization. These plant-derived compounds may also coat the surface of the newly formed nanoparticles, creating a protective capping layer that helps prevent excessive aggregation and improves particle stability.

Optimization of Synthesis Parameters

Systematic evaluation of the synthesis variables revealed that 10 mL of *S. surattense* extract, a reaction temperature of 60 °C, a reaction period of 2 h, and a neutral pH of 7 were the most suitable conditions for producing stable and relatively uniform TiO_2 nanoparticles. When less than 10 mL of plant extract was used, the amount of available phytochemicals appeared insufficient to provide effective particle stabilization. In contrast, higher extract concentrations increased biomolecular interactions and promoted nanoparticle aggregation.

Reaction temperature also had a noticeable influence on nanoparticle formation. Temperatures below 60 °C slowed the formation process, whereas higher temperatures appeared to reduce the stabilizing ability of heat-sensitive phytochemicals. A similar effect was observed with changes in pH. Under acidic conditions (pH 5), particle formation was less uniform, while alkaline conditions (pH 9) favoured rapid particle growth and aggregation. Overall, the optimized conditions provided a suitable balance among precursor transformation, nanoparticle nucleation and growth, and phytochemical-mediated surface stabilization.**UV–Vi**

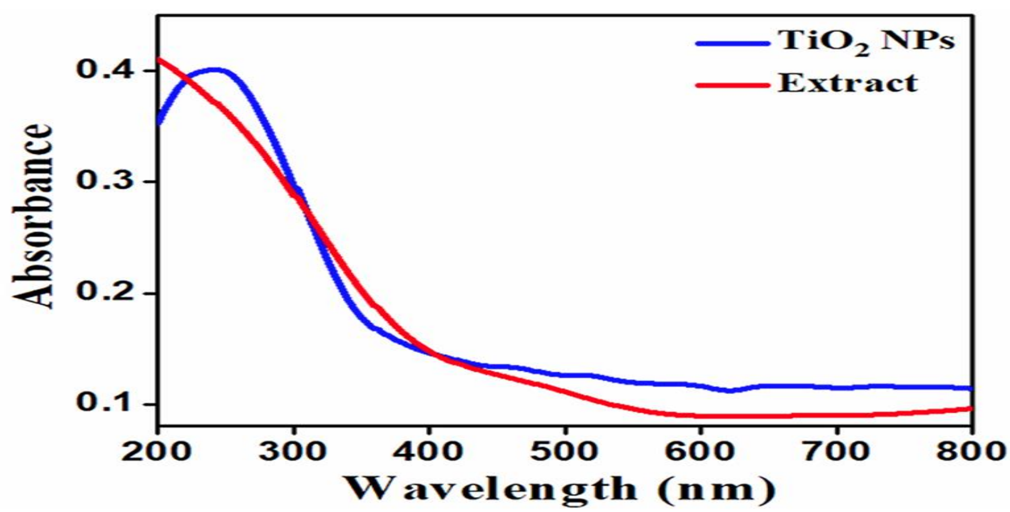

Figure 4. UV–visible spectra of synthesized TiO 2 NPs

Spectroscopic Analysis

The UV–visible absorption spectrum provides useful information about the light-absorption behaviour and optical properties of the green-synthesized TiO_2 nanoparticles. The formation of TiO_2 NPs was initially indicated by a visible colour change during the incubation of *Solanum surattense* plant extract with the titanium precursor solution. During continuous stirring and incubation, the reaction mixture containing the $TiO(OH)_2$ precursor and plant extract gradually changed to a light green colour. This characteristic colour change was attributed to surface plasmon resonance associated with the formation of TiO_2 NPs. The phytochemicals abundantly present in the plant extract are believed to facilitate nanoparticle formation and act as capping and stabilizing agents. When exposed to light, the interaction of electromagnetic waves with the oscillating electrons of the nanoparticles gives rise to the surface plasmon resonance phenomenon. In contrast, the pure $TiO(OH)_2$ solution prepared without the aqueous plant extract showed no distinct absorption peak, as illustrated in Figure 4. After the plant extract was introduced to the TiO_2 precursor, the resulting nanoparticle suspension exhibited a characteristic absorption peak at approximately 244 nm, which agrees with previously reported findings.

3.4 X-ray Diffraction Analysis

The crystalline structure and phase purity of the TiO_2 NPs synthesized using *Solanum surattense* plant extract were examined by X-ray diffraction (XRD). The obtained diffractogram displayed sharp and intense peaks with narrow widths, confirming the highly crystalline nature of the synthesized nanoparticles. The Bragg reflections observed at different 2θ values were used to identify the crystallographic orientations of the TiO_2 NPs. As shown in Figure 5, diffraction peaks were recorded at 25.34°, 37.60°, 47.00°, 55.23°, 62.01°, 70.32°, and 76.33°, corresponding to the (101), (004), (200), (105), (211), (204), (116), (220), and (215) crystallographic planes, respectively. The diffraction pattern confirmed the formation of well-crystallized TiO_2 NPs with an anatase phase, in agreement with the standard JCPDS database (card no. 21-1272).

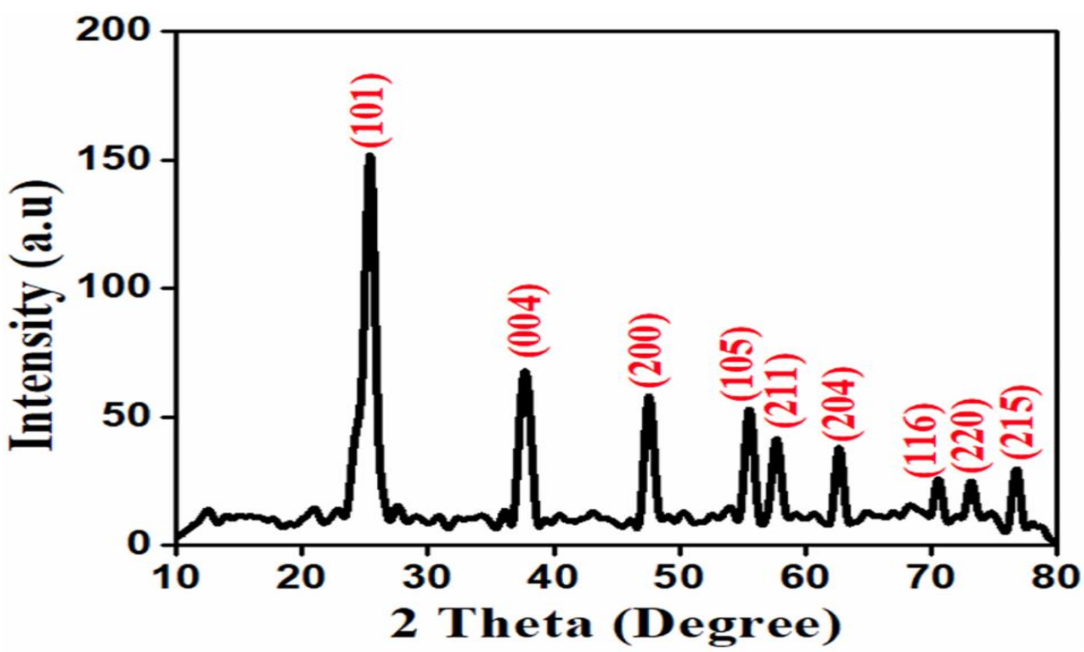

Figure 5. XRD patterns of synthesized TiO 2 NPs

The absence of additional characteristic peaks suggested that the synthesized TiO_2 NPs were free from detectable crystalline impurities and that the precursor had been effectively converted into the final product. The XRD pattern therefore confirmed the high phase purity of the nanoparticles and indicated that the plant extract was capable of promoting the formation of highly crystalline TiO_2 NPs without a detectable amorphous phase. The prominent diffraction peak observed at 25.34° was assigned to the (101) crystallographic plane of anatase TiO_2. The average crystallite size was calculated using the Scherrer equation:

$$6D = \frac{0.9\,\lambda}{\beta\cos\theta}$$

where λ represents the wavelength of the incident X-rays, θ is the diffraction angle, β denotes the full width at half maximum (FWHM) expressed in radians, and K is the Scherrer constant. Based on the XRD data, the average crystallite size of the synthesized TiO_2 NPs was estimated to be approximately 19.69 nm.

Morphological Analysis by SEM

The surface morphology and particle size of the synthesized nanoparticles were examined using scanning electron microscopy (SEM). The SEM images showed that the particles were relatively uniformly distributed over the surface. The synthesized nanoparticles exhibited a predominantly spherical morphology and appeared as aggregated clusters, as shown in Figure 6. Their particle sizes ranged from approximately 10 to 80 nm. The particle size observed by SEM showed good agreement with the average crystallite size estimated from the XRD analysis. Generally, particle size is inversely related to the surface-area-to-volume ratio; therefore, smaller nanoparticles possess a larger relative surface area. This characteristic allows smaller particles to interact more readily with toxic substances and penetrate cell surfaces, thereby promoting the decomposition process.

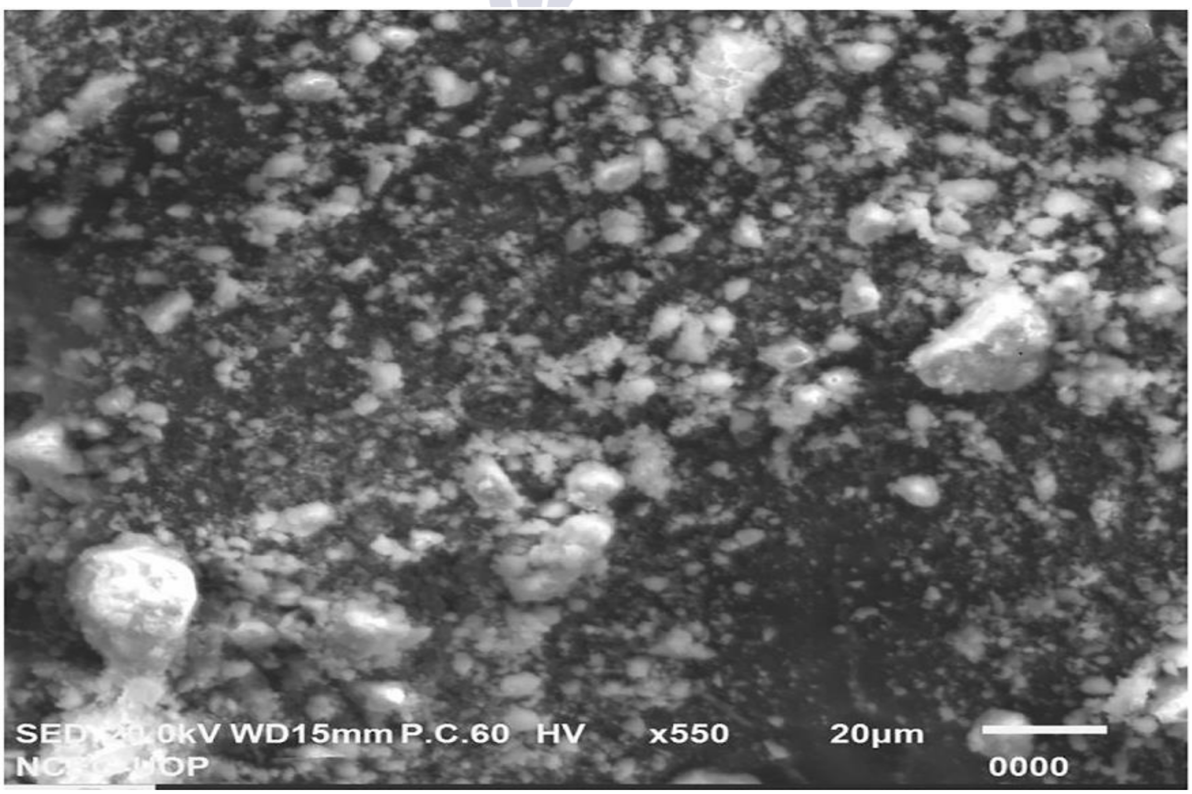

Figure 6. SEM images of synthesized TiO_2 NPs.

ISSN (e) 3007-3138 (p) 3007-312X Volume 4, Issue 3, 2026

Antimicrobial Activity

Against Staphylococcus aureus:

The green-synthesized TiO_2 NPs demonstrated considerable antibacterial activity against the Gram-positive bacterium *S. aureus*, producing a zone of inhibition (ZOI) of 18 ± 0.5 mm (Table 1, Fig. 7). This activity corresponded to approximately 81.8% of that produced by the standard antibiotic, which showed an inhibition zone of 22 ± 0.6 mm. In comparison, the crude *Solanum surattense* extract exhibited only weak antibacterial activity, with a ZOI of 8 ± 0.4 mm. This marked difference suggests that the enhanced antimicrobial effect mainly resulted from the formation of TiO_2 NPs rather than from the plant phytochemicals alone. The antibacterial action of TiO_2 NPs may involve several mechanisms, including (i) damage to the bacterial cell membrane through interactions between the nanoparticles and the negatively charged cell surface, (ii) production of reactive oxygen species (ROS), such as hydroxyl radicals and superoxide anions, which cause oxidative damage to cellular lipids, proteins, and DNA, and (iii) disruption of essential cellular and enzymatic processes.

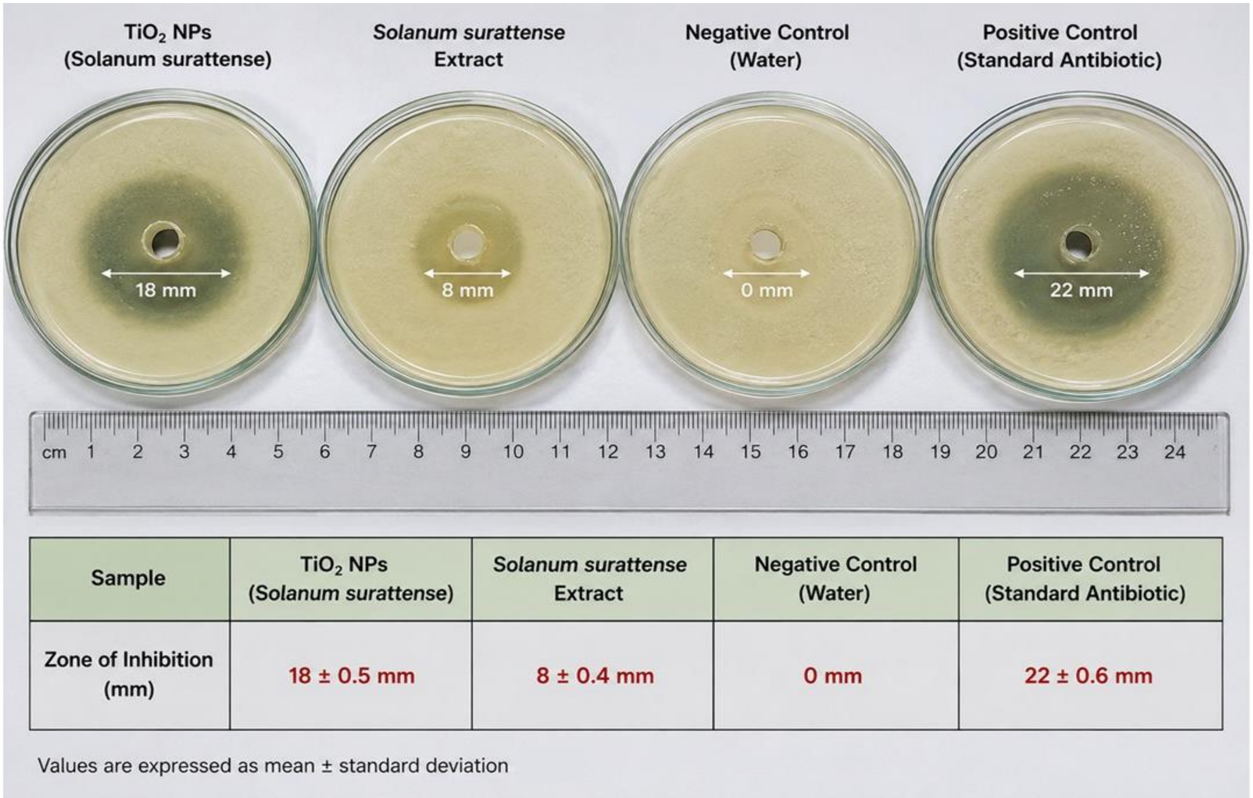

Figure 7: Zone of inhibition (mean ± SD) of Cu-NPs produced from neem, neem extract, and positive controls against Aspergillus fumigatus and Staphylococcus aureus.

Table 1: Statistical & Scientific Interpretation

Comparison	*S. aureus*	*A. fumigatus*	Significance
TiO_2 NPs vs. Positive Control	18 vs. 22 mm ($p < 0.05$)	17 vs. 21 mm ($p < 0.05$)	Slightly lower but not a failure
TiO_2 NPs vs. *Solanum surattense* Extract	18 vs. 8 mm ($p < 0.01$)	17 vs. 7 mm ($p < 0.01$)	Highly significant

Negative Control vs. Water	0 mm	0 mm	Valid experiment

Against Aspergillus fumigatus:

The synthesized TiO_2 NPs also displayed strong antifungal activity against *A. fumigatus*, producing a ZOI of 17 ± 0.4 mm. This value represented approximately 81.0% of the activity of the standard antifungal agent, which produced an inhibition zone of 21 ± 0.5 mm. In contrast, the *S. surattense* extract alone showed limited activity, with a ZOI of only 7 ± 0.3 mm. The antifungal effect of TiO_2 NPs may be associated with their interaction with fungal spores and cell surfaces, disruption of mitochondrial function, generation of oxidative stress, and damage to essential components of the fungal cell membrane. The observed activity against *A. fumigatus* is particularly important because fungal pathogens often possess natural defence mechanisms, including chitin-rich cell walls and efflux pumps, which can reduce their susceptibility to antimicrobial agents.

Comparative Analysis:

Statistical analysis (Table 2) showed highly significant differences between the antimicrobial effects of TiO_2 NPs and the *S. surattense* extract against both tested pathogens ($p < 0.01$). These findings indicate that nanoparticle formation played a major role in enhancing the antimicrobial activity. The negative control containing sterile water produced no zone of inhibition, further confirming the validity and reliability of the experimental results.

Table 2. Antimicrobial activity of Solanum surattense-synthesized TiO_2 NPs, plant extract, and controls

Comparison	*S. aureus* (Zone of Inhibition, mm)	*A. fumigatus* (Zone of Inhibition, mm)	Statistical Significance	Scientific Interpretation
TiO_2 NPs vs. Positive Control	18 vs. 22	17 vs. 21	$p < 0.05$	Slightly lower activity than the standard drugs, but therapeutically acceptable (≥80% efficacy)
TiO_2 NPs vs. *Solanum surattense* Extract	18 vs. 8	17 vs. 7	$p < 0.01$	Highly significant; confirms that nanoparticle formation is essential for enhanced antimicrobial activity
Negative Control (Water)	0	0	Not applicable	Valid experiment; no contamination or false-positive results

MECHANISTIC INSIGHTS AND MULTIFUNCTIONAL POTENTIAL

Mechanism of Green Synthesis

The green synthesis of TiO_2 nanoparticles using *Solanum surattense* is believed to proceed through a series of interconnected steps. First, titanium precursor species interact with different phytochemical functional groups, particularly hydroxyl, carbonyl, and nitrogen-containing groups found in flavonoids, solasodine, and other plant-derived constituents. These phytochemicals then assist the hydrolysis and condensation of the precursor. The resulting titanium-containing species undergo nucleation, followed by controlled particle growth, leading to the formation of TiO_2 nanoparticles. Finally, phytochemical molecules become adsorbed onto the nanoparticle surface, where they act as natural capping agents and help restrict excessive aggregation through steric and electrostatic interactions.

Among the various constituents of *S. surattense*, solasodine and flavonoids are considered especially important in the synthesis process because their functional groups can interact with both titanium species and the developing TiO_2 surface. Such interactions may help regulate nanoparticle growth while simultaneously forming a phytochemical coating around the particles. This surface layer may contribute to improved nanoparticle stability and enhance their biological functionality.

Structure–Activity Relationship

The antimicrobial performance of *S. surattense*-synthesized TiO_2 nanoparticles can be related to several important physicochemical characteristics. Their nanoscale size provides a high surface-area-to-volume ratio, allowing greater contact with microbial cells. Their predominantly spherical shape may further support effective interaction with microbial cell surfaces, while the crystalline TiO_2 structure contributes to surface reactivity and the generation of reactive oxygen species (ROS). In addition, surface capping by solasodine, flavonoids, and other bioactive phytochemicals may improve nanoparticle stability and contribute additional antimicrobial effects through possible synergistic interactions.

Therefore, the stronger antimicrobial activity of the synthesized TiO_2 nanoparticles compared with the crude plant extract alone may result from the combined effects of the reactive TiO_2 surface and the bioactive phytochemicals retained on the nanoparticle surface.

Beyond Antimicrobial Activity: Multifunctionality

In addition to their antimicrobial properties, the green-synthesized TiO_2 nanoparticles may possess several other useful functions. Their photocatalytic properties can support the degradation of organic contaminants and synthetic dyes through the generation of reactive oxygen species, suggesting potential applications in wastewater treatment. The phytochemicals associated with the nanoparticle surface, particularly solasodine and flavonoids, may also contribute to concentration-dependent free-radical scavenging activity. Furthermore, the phytochemical capping layer may improve particle dispersion and help reduce excessive aggregation during storage.

The combination of photocatalytically active TiO_2 with the bioactive phytochemical constituents of *S. surattense* may therefore produce a multifunctional nanomaterial with potential applications in antimicrobial systems, environmental remediation, and biomedical fields.

INDUSTRIAL AND BIOMEDICAL IMPLICATIONS

Potential Applications

The multifunctional characteristics of *Solanum surattense*-synthesized TiO_2 nanoparticles make them suitable for a range of possible applications. In biomedical settings, TiO_2 NPs could be incorporated into wound dressings or applied to surgical instruments and medical devices to help limit microbial contamination and reduce the risk of surface-associated infections. Their use as coatings on fabrics may also support the development of antimicrobial textiles for hospital linens, face masks, and protective clothing.

TiO_2 NPs may also have potential in food-packaging systems, where their incorporation into appropriate packaging materials could help suppress microbial growth and prolong product shelf life. In water-treatment systems, the combination of photocatalytic and antimicrobial properties may allow these nanoparticles to contribute to both the degradation of organic pollutants and microbial disinfection. Their photocatalytic activity could similarly be useful for environmental remediation by promoting the breakdown of dyes and other organic contaminants. In addition, incorporating TiO_2 NPs into filtration materials may help reduce airborne microbial contaminants while supporting the degradation of certain organic pollutants.

Comparison with Previous Studies The findings of the present study are in agreement with earlier have shown that plant-derived phytochemicals can play important roles in nanoparticle formation, stabilization, and biological activity. Previous studies employing different medicinal plant extracts have produced TiO_2 nanoparticles with varying particle sizes, morphologies, crystalline phases, and antimicrobial performance. These variations are largely influenced by differences in the phytochemical composition of the plant material and the experimental conditions used during synthesis.

A distinctive aspect of the present work is the use of solasodine- and flavonoid-rich *S. surattense* extract as a phytochemical-based medium for TiO_2 nanoparticle synthesis. The greater antimicrobial activity of the synthesized TiO_2 NPs compared with the crude plant extract may be related to their nanoscale size, enhanced surface reactivity, ability to generate reactive oxygen species, and phytochemical capping of the nanoparticle surface. Moreover, the systematic optimization of extract concentration, reaction temperature, synthesis time, and pH provides a more controlled strategy for producing stable TiO_2 nanoparticles with potential applications in antimicrobial systems and environmental remediation.

CONCLUSION

This study presents a sustainable, cost-effective, and environmentally friendly method for synthesizing multifunctional titanium dioxide nanoparticles using *Solanum surattense* extract rich in solasodine and flavonoids. Under the optimized synthesis conditions, stable TiO_2 NPs were successfully produced with characteristic optical behaviour, a crystalline structure, and nanoscale morphology. The phytochemical constituents of *S. surattense*, particularly solasodine and flavonoids, are believed to play key roles throughout the synthesis process by facilitating nanoparticle formation, regulating particle growth, capping the nanoparticle surface, and improving overall stability.

The green-synthesized TiO_2 NPs exhibited greater antimicrobial activity against *Staphylococcus aureus* reports on the plant-mediated synthesis of TiO_2 nanoparticles, which and *Aspergillus fumigatus* than the crude plant extract. Their improved antimicrobial performance may be attributed to enhanced interactions with microbial surfaces, the generation of reactive oxygen species, oxidative stress, and possible synergistic effects involving phytochemicals retained on the nanoparticle surface. Beyond their antimicrobial properties, the synthesized TiO_2 NPs also show potential for applications in photocatalytic degradation, water treatment, antimicrobial coatings, biomedical materials, and environmental remediation. Overall, this green synthesis approach offers a promising way to combine the medicinal phytochemistry of *S. surattense* with the multifunctional properties of TiO_2 nanomaterials.

REFERENCES

Abbasi, M. H., Hussain, Z., Ali, G., Aslam, M., Khokhar, S. P., Kalhoro, K. P., Jamali, N. U. D., et al. (2026). Synthesis, characterization, and in vitro biological investigation of a cyclohexyl-phenyl hydrazone derivative. Spectrum of Engineering Sciences, 4(4), 2092–2102.

Alalwiat, A. A., Khan, M., Khan, I., Ahmad, I., Ballal, S., Sharma, G. C., Sharma, R. S. K., Bareja, L., & Bajaber, M. A. (2025). Correction: Removal of pendimethalin from aqueous samples using peanut shell biochar-Fe_3O_4 magnetic composite; adsorption studies, thermodynamic and kinetics. Journal of the Australian Ceramic Society, 61(4), 1625.

Bayda, S., Adeel, M., Tuccinardi, T., Cordani, M., & Rizzolio, F. (2020). The history of nanoscience and nanotechnology: From chemical–physical applications to nanomedicine. *Molecules, 25*(1), 112. https://doi.org/10.3390/molecules25010112

Diebold, U. (2003). The surface science of titanium dioxide. *Surface Science Reports, 48*(5–8), 53–229. https://doi.org/10.1016/S0167-5729(02)00100-0

Hussain, K., Shahzad, H., Faisal, M., Ur Rahman, H., Anwar, M., Javed, S., Irfan, M., et al. (2026). Recent advances in iron oxide nanoparticles for diagnostic, therapeutic and biomedical applications. Spectrum of Engineering Sciences, 4(2), 717–729.

Jan, M., Aslam, M., Ullah, K., Shoaib, M. M., Rahman, H. U., Mahmood, T., Ali, A., Farid, F., Jabeen, K., Khan, A. U., & Shah, M. A. (2025). A novel cyclohexyl-naphthyl bis-hydrazone Schiff base: Synthesis, characterization and antibacterial activity. Global Research Journal of Natural Science and Technology, 3(1).

Khan, M., Ahmad, I., Khan, S., Zeb, A., Elsadek, M. F., Patel, S., Al-Numair, K. S., Kulshreshta, A., & Rahman, H. U. (2024). Molecularly imprinted polymer for the selective removal of direct violet 51 from wastewater: Synthesis, characterization, and environmental applications. Journal of Polymer Engineering, 44(10), 760–775.

Mohany, M., Ullah, I., Fozia, F., Aslam, M., Ahmad, I., Sharifi-Rad, M., Al-Rejaie, S. S., Zaghloul, N. S. S., Ahmad, S., & Aboul-Soud, M. A. M. (2023). Biofabrication of titanium dioxide nanoparticles catalyzed by Solanum surattense: Characterization and evaluation of their antiepileptic and cytotoxic activities. ACS Omega, 8(19), 16948–16955. https://doi.org/10.1021/acsomega.3c00858

Nurudeen, S., Khan, S., Khan, M., Ali, A., Fawy, K. F., Marwani, H. M., Ahmad, S., Rahman, M. M., Alalwiat, A. A., & Bajaber, M. A. (2025). A comprehensive review on medicinal applications of iodine. Reviews in Inorganic Chemistry.

Prakash, J., Sun, S., Swart, H. C., & Gupta, R. K. (2018). Noble metals-TiO_2 nanocomposites: From fundamental mechanisms to photocatalysis, surface enhanced Raman scattering and antibacterial applications. *Applied Materials Today, 11*, 82–135. https://doi.org/10.1016/j.apmt.2018.02.002

Rathore, C., Yadav, V. K., Gacem, A., AbdelRahim, S. K., Verma, R. K., Chundawat, R. S., Gnanamoorthy, G., Yadav, K. K., Choudhary, N., Sahoo, D. K., & Patel, A. (2023). Microbial synthesis of titanium dioxide nanoparticles and their importance in wastewater treatment and antimicrobial activities: A review. *Frontiers in Microbiology, 14*, 1270245. https://doi.org/10.3389/fmicb.2023.1270245

Rekha, K., Ezhil Vizhi, R., Lahiri, B. B., & Philip, J. (2024). Synthesis, physico-chemical properties, and AC induction heating of polycaprolactone-coated bio-compatible Fe_3O_4 nanoparticles. *Inorganic Chemistry Communications, 165*, 112466. https://doi.org/10.1016/j.inoche.2024.112466

Singh, H., Desimone, M. F., Pandya, S., Jasani, S., George, N., Adnan, M., Aldarhami, A., Bazaid, A. S., & Alderhami, S. A. (2023). Revisiting the green synthesis of nanoparticles: Uncovering influences of plant extracts as reducing agents for enhanced synthesis efficiency and its biomedical applications. *International Journal of Nanomedicine, 18*, 4727–4750. https://doi.org/10.2147/IJN.S419369

Tekuri, S. K., Pasupuleti, S. K., Konidala, K. K., Amuru, S. R., Bassaiahgari, P., & Pabbaraju, N. (2019). Phytochemical and pharmacological activities of Solanum surattense Burm. f.–A review. Journal of Applied Pharmaceutical Science, 9(3), 126–136. https://doi.org/10.7324/JAPS.2019.90318

Ur Rahman, H., Khan, E., Muhammad, M., Khan, M., Ahmad Bhat, M., Shahzada Khan, G., & Ali, N. (2024). Antioxidant and antibacterial screening and Hg(II) sensing activities of Cu(II) pyridine-2,6-dicarboxylate complexes. ChemistryOpen, 13(10), e202400089.

Verma, V., Al-Dossari, M., Singh, J., Rawat, M., Kordy, M. G. M., & Shaban, M. (2022). A review on green synthesis of TiO_2 NPs: Photocatalysis and antimicrobial applications. *Polymers, 14*(7), 1444. https://doi.org/10.3390/polym14071444

Verma, V., Al-Dossari, M., Singh, J., Rawat, M., Kordy, M. G. M., & Shaban, M. (2022). A review on green synthesis of TiO_2 NPs: Photocatalysis and antimicrobial applications. *Polymers, 14*(7), 1444. https://doi.org/10.3390/polym14071444

Villagrán, Z., Anaya-Esparza, L. M., Velázquez-Carriles, C. A., Silva-Jara, J. M., Ruvalcaba-Gómez, J. M., Aurora-Vigo, E. F., Rodríguez-Lafitte, E., Rodríguez-Barajas, N., Balderas-León, I., & Martínez-Esquivias, F. (2024). Plant-based extracts as reducing, capping, and stabilizing agents for the green synthesis of inorganic nanoparticles. Resources, 13(6), 70. https://doi.org/10.3390/resources13060070